Journal of Power Sources 195 (2010) 1936–1939

Contents lists available at ScienceDirect

Journal of Power Sources

journal homepage: www.elsevier.com/locate/jpowsour

Short communication

# Structure of porous electrodes in polymer electrolyte membrane fuel cells: An optical reconstruction technique

Viatcheslav Berejnov*, David Sinton, Ned Djilali

*Department of Mechanical Engineering and Institute for Integrated Energy Systems, University of Victoria, Victoria, V8W 3P6, Canada*

ARTICLE INFO

*Article history:*
Received 9 September 2009
Received in revised form 15 October 2009
Accepted 16 October 2009
Available online 29 October 2009

*Keywords:*
Fibrous porous electrode
Gas diffusion layer
Porous transport layer
Three-dimensional structure
Image reconstruction

ABSTRACT

Computing flows and phase transport in porous media requires a physically representative geometric model. We present a simple method of digitizing the structure of fibrous porous media commonly used in polymer electrolyte membrane (PEM) fuel cells, the so-called gas diffusion layer (GDL). Employing an inverted microscope and image recognition software we process images of the GDL surface collected manually at different focal lengths with micrometer accuracy. Processing the series of images allows retrieval of local depths of the salient in-focus structural elements in each of the different images. These elements are then recombined into a depth-map representing the three-dimensional structure of the GDL surface. Superimposition of the in-focus portions of the structural elements distributed throughout the stack of images yields digitized data describing the geometry and structural attributes of the 3D surface of the GDL fibrous material.

© 2009 Elsevier B.V. All rights reserved.

## 1. Introduction

Characterization of transport properties within porous media is becoming increasingly dependent on computational methods. Because of their nature, these methods utilize a digital representation of the porous media. The numerical modelling of geometric elements representing the real porous material is a well established practice for obtaining the digital porous structures [1–3]. Such methods superimpose the geometrical elements into a continuous (periodic) network employing different hypotheses of superposition. However, the somewhat *ad hoc* structures obtained by numerical models should be considered as *artificial* in the sense that the geometric superposition is somewhat *ad hoc* and resulting structures are not an *exact* representation of the *real* porous material.

The gap between artificial and natural digital porous structures leads to uncertainties and incomplete understanding on how the specific details of the porous structure affect multiphase transport for instance. Indeed, the difference between the artificial and natural structures may not be obvious at first glance, and could result in discrepancies between computed and actual imbibition/drainage regimes. A more accurate digital representation of the real porous media could therefore lead to more accurate theoretical modelling and predictions. In this context, the possibility of identifying the structure of water transport pathways/network over larger portions of a GDL using a fast, sufficiently sensitive and inexpensive method would be particularly useful.

Recently, it was demonstrated that the methods based on X-ray micro-tomography could provide structural digital information of fibrous porous media with sufficient accuracy [4–8]. However, in spite of its many advantages, X-ray micro-tomography requires an expensive specialized facility that limits its applicability. In this paper we propose an alternative technique which only requires standard optical microscopy complemented by modern image processing algorithms. Our method is able to provide detailed and almost 3D displays of large areas of a GDL sheet, and is thus a good potential complement to slower and much more expensive tomography techniques.

Three-dimensional object cannot be fully represented by a single optical image (not a hologram) recording an intensity modulation without loosing a noticeable amount of information about the 3D shape. However, recording an object using a series of optical images can indeed preserve the information on its 3D geometry by distributing this information through all the images making up the recorded series. There are two ways to go about this recording: either consecutively sweeping a focal distance or moving the object through the constantly set focal plane. The application of special algorithms to this image series allows retrieval of the object's shape and reconstruction of the 3D profile.

All the image reconstruction methods discussed in literature can be distinguished by processing the difference between two consecutively recorded images and can generally be placed between

* Corresponding author at: Institute for Integrated Energy Systems, University of Victoria, PO Box 3055 STN CSC, Victoria, BC, V8W 3P6 Canada Tel.: +1 250 385 0209; fax: +1 250 721 6323.
*E-mail address:* berejnov@gmail.com (V. Berejnov).

0378-7753/$ – see front matter © 2009 Elsevier B.V. All rights reserved.
doi:10.1016/j.jpowsour.2009.10.050

two extremes [9,10]. The first category consists of the convolution methods [11–18] employing the blur portions of an image for constructing the depth-map of the original object. In contrast, the second category [19–25] uses the sharp portions instead subtracting those sharp portions from the image stack and fusing them upon the different filtering algorithms. As a result, the first category requires only a limited number of the images and a perfectly calibrated optical system outputting the three-dimensional image with a poorly textured surface. The second category is much less picky for the optical calibration; it operates with a large number of the images and can easily output the coarsely textured three-dimensional surface. In practice, the second category perfectly fits the conditions for imaging the surfaces of the fibrous porous materials that have both the microstructured texture and well developed micro-relief. Various common microscopes operating with either the common bright-field, fluorescent, or confocal optical schemas can effectively acquire the images suitable for these fusion algorithms. Higher resolution techniques such as AFM, are not considered here because the focus is the structure of the porous medium, rather than that of the individual fibers in the GDL.

The standard microscopy based reconstruction method is demonstrated in this paper by using an inexpensive bright-field microscope and low cost image processing software. A rapid method was developed to allow construction of digital images of highly irregular porous textured surfaces. The technique employs a manually operated upright optical microscope Leica DM LM with a combination of Helicon Focus (HF) software as an image processing unit. The HF based processing is found suitable and can deliver a reasonably accurate 3D shape of very complex fibrous structures [26]. We believe the method can be of benefit in both laboratory work and for material quality control in mass production.

## 2. Experimental and materials

In our experiments we used the Toray carbon paper B-2/060/40WP from E-TEK Company, USA [27] as a sample of the porous fibrous material. The thickness of the sheet of this carbon paper was ~200 μm and the diameter of the carbon filament was about 8 μm. The carbon paper samples measuring 2.5 cm × 2.5 cm were mounted horizontally on the Leica DM LM microscope stage. The microscope was used in the inverted mode. The resolution of positioning in the *X*–*Y* plain was 0.1 mm. The positions of the stage along the *Z*-axis were set by the microscope focal wheel with the micron scale calibrations for two intervals: 1 or 4 μm at 0.5 μm of accuracy . The series of the multi-focus images for a given view area were taken by varying the position of the stage along the *Z*-axis within the 4 μm interval and then processed with the HF software.

For the light sources we used a combination of a mercury lamp and an external diffusive light source mounted directly on the microscope objective. The external light source has a circular geometry and contains eight white-LEDs. We used the microscope objective 10×/0.30 HC PL Fluotar, Leica, Germany. The 8-bit images were captured with a Retiga 1300i black/white camera and preprocessed with the software QCapture Pro 6.0 from QCapture Inc.

## 3. Method

### 3.1. Basics of image reconstruction

A portion of the micro-sample surface that does not belong to the optical plane appears unfocused in an image recorded through the microscope objective, whereas an image portion positioned in the optical plane is focused well. This blurring effect obviously makes an interpretation of the surface texture difficult and uncertain. The reason for this uncertainty lies in the rather small value of the depth-of-field, DOF, for the microscope objectives [26]. The DOF can be understood as the thickness of an imaginary layer including an optical plane in the middle and positioned at a certain distance from the objective surface; all the sample surface's elements included in the DOF look focused. The DOF is a function of the objective lenses and the light wavelength and could be roughly estimated [28,29] as

$$\mathrm{DOF} \approx \frac{\lambda}{Na^2},$$

where λ is a wavelength of light that can be estimated as ~0.65 μm, and *Na* is the numerical aperture of the objective. The typical microscope objectives (first number is the magnification and second one is *Na*): 5 × 0.15, 10 × 0.30, 20 × 0.40, and 50 × 0.50 provide the following values of the DOFs: 29 μm, 7.2 μm, 4.1 μm, and 2.6 μm, respectively.

The small DOF of the microscope objective is a source of the poor focusing capability over the whole attainable sample depth. However, the small DOF can be turned into a powerful advantage with the help of modern image analysis algorithms. The small value of the DOF allows sweeping of the sample though the objective focal plane, sequentially recording images of the sample surface. The output of this acquisition is a stack of images in which every image contains different portions of the sharp and blurred aspects of the recorded sample surface. These stack of images are indexed with respect to the position to the focal plane.

### 3.2. Image acquisition and processing

The method employed recording of the multiple images in sequence as the sample surface was moved through the objectives focal plane. The images were arranged to overlap the whole attainable depth-profile of the sample surface. For the purpose of demonstrating the technique, and in order to restrict the number of manually acquired images to a reasonable number while spanning ~100 μm across the GDL, a DOF of 7.2 μm was used to acquire the data presented in this paper. With this setting 28 images [100/(DOF/2)] are required to span the 100 μm height. In fact 25 images were used. Other DOF values can be used and are documented in Ref. [26], and it should be noted that the DOF does not directly correlate with resolution, and better resolution that the DOF can in fact be achieved [26].

The image stack was then processed by the Helicon Focus software [30]. HF selected the in-focus portion of the sample surface from each image in the stack. It superimposed all the in-focus portions combining them into a single image and outputted a new, synthetic 2D image of the original surface that was sharp everywhere. Essentially, HF extended the DOF over the whole attainable relief of the sample, creating a focused image over the whole of the sample's surface.

Operating with the image stack, the HF software constructed a map of the depths/altitudes (defined arbitrarily) for those surface elements that could be processed and distinguished as being the in focus elements. This depth-map represents the 3D profile of the sample's surface relief. HF approximated the depth-map and outputted the 3D surface of the sample interface in the OBJ format suitable for numerical applications [26].

### 3.3. Calibration of the reconstruction method

Digitizing the surface of a sample involves multiple processing steps. Therefore it is a matter of interest to estimate the accuracy of the reconstruction process. The general idea here is to measure and compare the test objects in two ways: by measuring the object

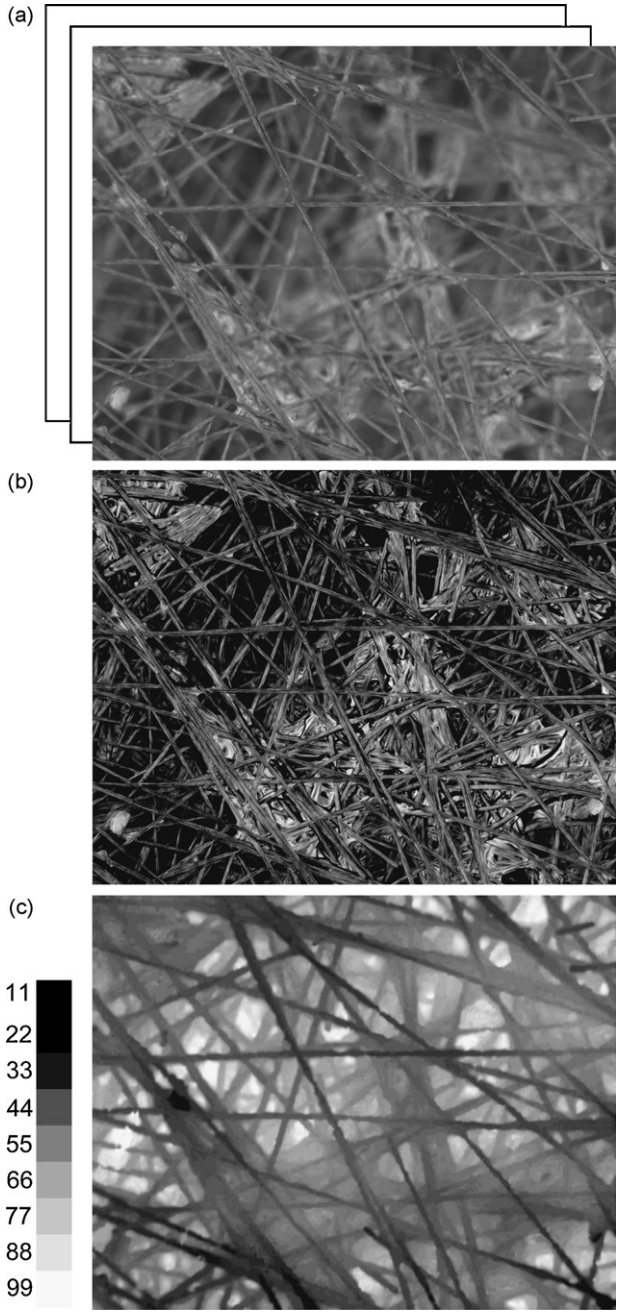


**Fig. 1.** The method of obtaining the structural data by processing the stack of images (a) with the Helicon Focus software; all images are recorded for different stage positions with respect to the microscope objective. The resultant image (b) contains only the in-focus portions numerically superimposed. The depth-map image (c) represents the local depths for the all pixels of the resultant image (b) with respect to an arbitrarily chosen zero-level image within the stack; the coding is done in the grey color scale at left representing the pixel's depth in μm.

directly and after the 3D reconstruction. This calibration procedure was performed with two sample objects [26]. One was an inclined optical calibration standard from Leica: a flat microscope slide with a 2 mm grid scale with 10 μm tick marks resolution. For the second sample, noting that the calibration procedure does not require an object having the same scales as the GDL fibers, but simply a well defined 3D surface providing the entire range of surface depth variations (*Z*-direction) relevant to GDL applications (i.e. 0–100 μm), a metal wavy copper mesh consisting of 100 × 100 meshes per square inch and wire of 0.0114 cm diameter was found to fit the requirements perfectly. The objective was 10 × 0.30 with

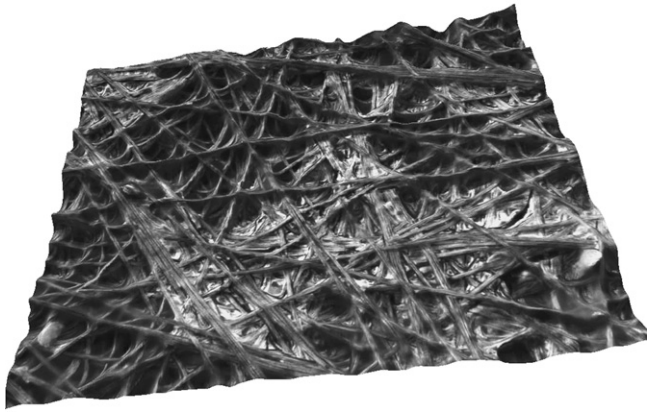

**Fig. 2.** 3D surface of fibrous carbon paper constructed by Helicon Focus software. This surface is an approximation of the 3D projection of the depth-map image presented in Fig. 1(c).

an image size of 1300 × 1030 pixels, the resolution in the *X*–*Y* plane is 1.5 pixels $\mu m^{-1}$. The HF software was able to reconstruct an element having a height of 100 μm with 1–2% accuracy [26].

## 4. Results

Fig. 1(a) represents a stack of the acquired raw images with a typical example up front. It is clearly seen that the fibrous structure in this image consists of both the blurred and in-focus portions. The areas of both those portions depend upon the particular 3D structural profile of the sample surface. The structural elements that are blurred in Fig. 1(a) are perfectly in focus in the other images in this stack and vice versa.

Employing the HF software and the stack of raw images we construct a synthetic image containing only the focused image parts (Fig. 1(b)). On this panel we can distinguish the important structural elements of the carbon paper. Particularly, panel (b) of Fig. 1 demonstrates a combination of two overlapping networks: the carbon fiber network and the binding web network. The two distinct structures, the fibers and webs, are well recognizable. Every pixel of Fig. 1(b) also has an index of its parent image in the image stack from which the pixel was gathered. The panel (c) in Fig. 1 represents only information from those indexes.

Because every two images in the stack are separated by 4 μm along the *Z*-axis we could turn an array of the image indexes into an array of the depths, representing how far the particular image is from the arbitrarily chosen top image (Fig. 1(a)). The panel in Fig. 1(c) visualizes the 3D profile of the carbon paper's texture recorded in the image stack of Fig. 1(a) and processed in Fig. 1(b). The white areas in the image presented in Fig. 1(c) indicate the bottom parts of the deep wells with depths of ~100 μm measured from the sample surface. We take the zero-level of the sample surface from the black fibers in Fig. 1(c), those fibers are closest to the microscope objective. Approximating the depth-map presented in panel (c) the HF software constructs the 3D surface of the examined fibrous sample (Fig. 2). Although the reconstruction spans the entire 100 μm depth of the GDL, the 3D perspective rendering in the figure allows visualization of near surface layers only. Close examination of the reconstructed image in Fig. 2 shows a slight waviness in the fiber. This is due to both the resolution and the 3D reconstruction algorithm. The 3D surface is not exact in the sense that the raw data was filtered and approximated by the algorithm using a polynomial spline 3D surface (the exact method is not disclosed by HF, the software supplier). The waviness indicates small discrepancies between the particular approximation function and the spatial sampling of the chosen

data set. This can be remedied by refining the choice of approximation function by for example recognizing the long side of the fiber and decreasing the degree of the polynomial along that direction. At the current proof and concept stage the output of the HF software is reasonable and sufficient to demonstrate the functionality of the method.

## 5. Conclusion

Using a simple manually operated microscope and inexpensive software we developed a method for rapidly constructing the 3D surface of fibrous porous media. The method consisted of two major steps: (1) acquiring the series of images from a sample through the sequential movement of the microscope stage and (2) applying the Helicon Focus software to the image stack. The HF software generated the sharp synthetic image of the whole attainable sample's profile and the 3D surface of the measured sample interface.

We found this method to be very convenient for inspecting, digitizing, and characterizing the microstructured surface of fibrous carbon papers.

## Acknowledgements

The authors benefitted from helpful discussions and input form Sanjiv Kumar (Ballard Power Systems) during the course of this work. The work was supported by the Canada Research Chairs program.

## References

[1] V.P. Schulz, J. Becker, A. Wiegmann, P.P. Mukherjee, C.Y. Wang, J. Electrochem. Soc. 154 (2007) B419–B426.
[2] G. Inoue, T. Yoshimoto, Y. Matsukuma, M. Minemoto, J. Power Sources 175 (2008) 145–158.
[3] Fraunhofer ITWM, 2009, http://www.geodict.com/.
[4] H.J. Vogel, J. Tolke, V.P. Schulz, M. Krafczyk, K. Roth, Vadose Zone J. 4 (2005) 380–388.
[5] T. Koido, T. Furusawa, K. Moriyama, J. Power Sources 175 (2008) 127–136.
[6] G. van Dalen, P. Nootenboom, L.J. van Vliet, L. Voortman, E. Esveld, Image Anal. Stereol. 26 (2007) 169–177.
[7] J. Becker, V. Schulz, A. Wiegmann, J. Fuel Cell Sci. Technol. 5 (2008).
[8] J.R. Izzo, A.S. Joshi, K.N. Grew, W.K.S. Chiu, A. Tkachuk, S.H. Wang, W.B. Yun, J. Electrochem. Soc. 155 (2008) B504–B508.
[9] A.G. Valdecasas, D. Marshall, J.M. Becerra, J.J. Terrero, Micron 32 (2001) 559–569.
[10] N. Bonnet, Micron 35 (2004) 635–653.
[11] J. Ens, P. Lawrence, IEEE Trans. Pattern Anal. Mach. Intell. 15 (1993) 97–108.
[12] M. Subbarao, G. Surya, Int. J. Comput. Vis. 13 (1994) 271–294.
[13] M. Subbarao, T.C. Wei, G. Surya, IEEE Trans. Image Process. 4 (1995) 1613–1628.
[14] J.W. Shaevitz, D.A. Fletcher, J. Opt. Soc. Am. A: Opt. Image Sci. Vis. 24 (2007) 2622–2627.
[15] V.P. Namboodiri, S. Chaudhuri, Pattern Recogn. Lett. 28 (2007) 311–319.
[16] J. Moon, S.Y. Park, Opt. Eng. 46 (2007).
[17] F. Aguet, D.V. De Ville, M. Unser, IEEE Trans. Image Process. 17 (2008) 1144–1153.
[18] J.G. McNally, T. Karpova, J. Cooper, J.A. Conchello, Methods-A: Companion Methods Enzymol. 19 (1999) 373–385.
[19] B. Forster, D. Van de Ville, J. Berent, D. Sage, M. Unser, Microsc. Res. Tech. 65 (2004) 33–42.
[20] S. Gabarda, G. Cristobal, Pattern Recogn. Lett. 26 (2005) 2572–2578.
[21] A. Punge, S.O. Rizzoli, R. Jahn, J.D. Wildanger, L. Meyer, A. Schonle, L. Kastrup, S.W. Hell, Microsc. Res. Tech. 71 (2008) 644–650.
[22] J. Meneses, M.A. Suarez, J. Braga, T. Gharbi, Appl. Opt. 47 (2008) 169–178.
[23] T.T.E. Yeo, S.H. Ong, Jayasooriah, R. Sinniah, Image Vis. Comput. 11 (1993) 629–639.
[24] H. Li, B.S. Manjunath, S.K. Mitra, Graph. Models Image Process. 57 (1995) 235–245.
[25] S.C. Lee, P. Bajcsy, Comput. Vis. Image Underst. 110 (2008) 19–31.
[26] V.V. Berejnov, arXiv.org, 2009, http://arxiv.org/abs/0904.2024.
[27] Toray Inc., 2009, http://fuelcellstore.com/products/toray/specs.pdf.
[28] G.A. Boutry, Instrumental Optics, 2nd ed., Interscience Publishers Inc., New York, 1962.
[29] R.J. Bracey, The Technique of Optical Instrument Design, 1st ed., The English Universities Press Ltd., London, 1960.
[30] Helicon Soft Ltd., 2009, http://www.heliconsoft.com/heliconfocus.html.